ELSEVIER

Biophysical Chemistry 114 (2005) 261–271

Biophysical Chemistry

http://www.elsevier.com/locate/biophyschem

Sequestering of p53 into DNA–protein filaments revealed by electron microscopy

Dmitry I. Cherny[a,b,1], Marie Brázdova[c,2], Jan Paleček[c,3], Emil Paleček[c], Thomas M. Jovin[a,*]

[a]*Max Planck Institute for Biophysical Chemistry, Göttingen, Germany*
[b]*Institute of Molecular Genetics, Russian Academy of Sciences, Kurchatov's Square, Moscow, Russia*
[c]*Institute of Biophysics, Academy of Science of the Czech Republic, 61265 Brno, Czech Republic*

Received 10 September 2004; received in revised form 17 December 2004; accepted 17 December 2004
Available online 18 January 2005

Abstract

Using electron microscopy, we analyzed the interaction of bacterially expressed full-length p53, p53(1–393), and its C-terminal fragment, p53(320–393), with long (~3000 bp) dsDNA in linear and supercoiled ($|\Delta Lk| \approx 4$–6) forms containing or lacking the p53 recognition sequence (p53CON). The main structural feature of the complexes formed by either protein was a DNA–protein filament, in which two DNA duplexes are linked (synapsed) via bound protein tetramers. The efficiency of the synapse, reflected in its length and the fraction of molecules exhibiting DNA–protein filaments, was significantly modulated by the molecular form of the protein and the topological state of the DNA. With linear DNA, the synapse yield promoted by the C-terminus fragment was very low, but the full-length protein was effective in linking noncontiguous duplexes, leading to the formation of intramolecular loops constrained at their bases by short regions of synapsed DNA duplexes. When the linear DNA contained p53CON, regions of preferential sequence, i.e., encompassing p53CON and probably p53CON-like sequences, were predominantly synapsed, indicating a sequence specificity of the p53 core domain. With scDNA, the synapse yield was significantly higher compared to the linear counterparts and was weakly dependent on the sign of superhelicity and presence or absence of p53CON. However, the full-length protein was more effective in promoting DNA synapses compared to the C-terminal fragment. The overall structure of the DNA–protein filaments was apparently similar for either protein form, although the apparent width differed slightly (~7–9 nm and ~10–12 nm for p53(320–393) and p53(1–393), respectively). No distortion of the DNA helices involved in the synapse was found. We conclude that the structural similarity of DNA–protein filaments observed for both proteins is attributable mainly to the C-terminus, and that the yield is dictated by the specific and possibly nonspecific interactions[4] of the core domain in combination with DNA topology. Possible implications for the sequestering of p53 in DNA–protein filaments are discussed.

Keywords: p53; Electron microscopy; DNA–protein complex; DNA–protein filaments; Oligomerization

1. Introduction

The p53 tumor suppressor protein plays an essential role in maintaining cell integrity in response to various forms of cellular stress [1,2]. p53 exerts an influence on numerous cellular processes, of which regulation of transcription is thought to be the most important. The key element of the p53 transcription regulation is its sequence-specific interaction with the p53 responsive elements (PRE) localized in the regulatory regions of the target genes [3]. Interaction between p53 and PRE is mainly determined by the structure of both the protein and the PRE.

* Corresponding author. Tel.: +49 551 2011382; fax: +49 551 2011467.
E-mail address: tjovin@gwdg.de (T.M. Jovin).
[1] Department of Biochemistry, University of Leicester, University Road, Leicester LEI 7RH, United Kingdom.
[2] Current address: Heinrich-Pette-Institut für Experimentelle Virologie und Immunologie, Universität Hamburg, Martinistrasse 52, Hamburg D-20251.
[3] Current address: Genome Damage and Stability Centre, University of Sussex, Brighton, BN1 9RQ, United Kingdom.
[4] The terms "specific binding" or "specific interaction(s)" were used exclusively in reference to sequence-specific processes. The term "nonspecific" denotes a non-sequence-specific mode of interaction.

0301-4622/$ - see front matter © 2004 Elsevier B.V. All rights reserved.
doi:10.1016/j.bpc.2004.12.042

p53 exhibits a functional and structural (domain) organization [2,4–10]: an acidic N-terminal transactivation domain (residues 1– ~70); a proline-rich domain (residues 60–97); a hydrophobic core domain (~100–300); an oligomerization domain (320–360) and a basic C-terminal domain (360–393). Specific DNA-binding activity is mainly determined by the core domain, although the C-terminus also binds DNA, albeit nonspecifically. Specific interactions with PRE (in response to stress) require post-translational modifications, i.e., phosphorylation and/or acetylation, of the full-length protein [1,5,7,11–13].

The full-length protein adopts a modular conformation with a defined structure for the core domain [14–16] and large unstructured regions located in the N- and C-terminal domains [16,17]. The latter property implies flexibility of p53 interactions with various proteins (and with itself as well) and DNA and structural plasticity of the complexes, reflected, for example, in its ability to form amyloid-like structures [18,19].

In solution, full-length p53 is a tetramer constituting the dominant functional form interacting with PRE [9]. However, higher order aggregates are found in solution and in a bound state [20,21]. p53 segments lacking the tetramerization domain but containing the core domain also bind PRE either as four distinct subunits [22] or as a multimeric complex [20,23].

The structure of PREs is highly variable. The common feature is presumed to be a decamer target 5′-PuPuPuC(A/T)(T/A)GPyPyPy-3′ (two head-to-head quarter sites; Pu, purines, and Py, pyrimidines) [14,21,24–26], with two consecutive decamers constituting the consensus sequence. The relative orientation of the two decamers is of little consequence for p53-specific binding, although a head-to-tail orientation enhances the binding efficiency [24,27]. Two decamers separated by up to 21 base pairs are still recognized by p53 [21,24,25,28]. Computer analysis of the known PREs has led to the concept of an extended version of that consensus sequence flanked by two additional nucleotides [29]. Furthermore, recent studies show that p53 can efficiently recognize other sites deviating significantly from the consensus sequence [30].

p53 also interacts with various irregular DNA structures, such as mismatches [31,32], Holliday junctions [33], protruding long ssDNA ends [34–36], cruciforms [37], t-loop junctions [38] and sequences adopting a non B-form conformation [39–41]. Mazur et al. [42] suggested that p53 binds to DNA crossovers in supercoiled DNA. Furthermore, it has been shown that various molecular forms of p53 bind more efficiently to scDNA relative to linear molecules [43–46].

The variety of p53 DNA-binding activities, the structural plasticity and oligomeric state of the full-length protein, and the wide diversity of the recognition sequence imply a high degree of complexity in the interactions of p53 with DNA, which should be reflected in the structure of the diverse complexes. Surprisingly, bound p53 imaged by electron microscopy (EM) or scanning probe microscopy is mainly globular in shape, regardless of the nature of the protein used and the structure of the nucleic acid [20,23,31,33–38,41,43,47–49]. However, recent data indicated that certain C-terminal segments of p53 lacking the core binding domain interact preferably with scDNA in a sc/linear DNA competition assay, leading to the formation of a DNA–protein filaments in which distant (opposing) DNA duplexes are linked (synapsed) via bound protein dimers or tetramers [46].

In order to establish whether formation of DNA–protein filaments was exclusively limited to the C-terminal fragments, we analyzed the interaction of bacterially expressed full-length p53 and its C-terminal fragment with linear and supercoiled DNA with and without p53CON. The data demonstrate that DNA–protein filaments are characteristics of the full-length protein as well, thus implying a role of the C-terminus in determining the structure of these complexes. However, specific and possibly nonspecific interactions of the core domain together with DNA topology contribute significantly to the yield of DNA–protein filaments.

2. Materials and methods

2.1. DNA

Negatively supercoiled pBluescript SK II+ DNA (2961 base pairs) and pPGM1 DNA plasmid derived from pBluescript SK II+ DNA by cloning the p53 20-mer recognition sequence 5′-AGACATGCCTAGACATGCCT-3′ (p53CON) into the *Hind*III site [43] were purified using Qiagen kits (Qiagen, Germany). Negatively and positively supercoiled DNAs with a reduced number of superhelical turns ($|\Delta Lk| \approx 4$–6) were obtained and characterized as described [50]. A double-stranded (ds) duplex was obtained by annealing HPLC-purified oligonucleotides 5′-GCTTGCATGCCAGTTTTCTTCTTCTGCAGGTC-GAC-3′ and 5′-GTCGACCTGCAGAAGAAGAAA-ACTGGCATGCAAGC-3′ (Metabion, Germany) in 10 mM Na–Cacodylate, pH 7.0, 100 mM NaCl and used without further purification. The yield and quality of the ds oligonucleotide were analyzed by 10% native PAGE (30:1 in acrylamide:bisacrylamide).

2.2. Purification and characterization of p53 proteins

Bacterially expressed full-length protein, p53(1–393), was prepared and characterized according to [45]. The C-terminal fragment, p53(320–393), was purified according to [51]. The purity and size of the proteins were assessed by SDS–PAGE [46]. The proteins were homogeneous in size, free of detectable contaminations (proteins) of smaller or larger molecular weight and exhibited a tetrameric organization [45,46].

2.3. Preparation of DNA–protein complexes

Complexes of p53 with DNA and ds oligonucleotides were formed in a buffer containing 10 mM Na–HEPES, pH 7.5, 50 mM KCl, 0.01% Triton X-100 in a total volume of 10–20 μL. The DNA concentration was 2–8 μg/ml. The molar protein/DNA ratios were calculated for tetrameric protein units and are indicated in the text and figure legends. Complexes with the ds oligonucleotide were prepared by incubation of 3 μM protein with 0.1 μM of DNA duplex. Samples were incubated in ice for 30–60 min, and aliquots were withdrawn for EM sample preparation.

2.4. Electron microscopy

The general procedure for preparing electron microscopy samples was as follows: an aliquot of 1–2 μl was withdrawn from the incubation mixture and diluted in 10 mM Na–HEPES, pH 7.5, 10 mM KCl to a final DNA concentration of 0.2–0.5 μg/ml. 10–15 μL of the diluted mixture was placed onto a carbon film attached to an EM grid (in some experiments a drop was placed onto a Parafilm sheet and immediately covered with an EM grid coated with a carbon film; no difference in complex structures and their yield was found by either procedure). Glow-discharged carbon films were prepared as described [23]. The adsorption continued for 1–2 min, after which the grids were rinsed with a few drops of 2% aqueous uranyl acetate, blotted with filter paper and dried. The samples were observed with a Philips CM12 electron microscope in a tilted dark-field mode. The negatives were scanned with an Agfa Duoscan 2500 scanner at 1200 dpi. DNA lengths were measured with NIH image modified for Windows (Scion, release beta 3). For printing, images were flattened using a high-pass filter with a radius of 250 pixels and subsequently adjusted for contrast/brightness using Adobe Photoshop.

2.5. Alignment of the molecules

The analysis of the complexes formed by p53(1–363) with linear DNA was as follows: we measured the lengths of DNA loops, free DNA segments and synapsed DNA and calculated the coordinates for all duplex crossovers, i.e., at the beginning and the end of synapses. In the major fraction of DNA molecules, at least one duplex crossover determined in this procedure was located very closely to one DNA end (pPGM1/*Eco*RI) and at ~40% from one DNA end (pPGM1/*Sca*I DNAs), corresponding to the position of p53CON. We concluded that a major fraction of loops had arisen from at least one specific binding of p53(1–363) to p53CON and this complex was used as a marker for the unambiguous alignment of the molecules. From the entire population of molecules, we selected those containing at least one loop formed by the specifically bound protein. The final histograms were plotted such that the most prominent peaks corresponding to the binding to the p53CON were placed at the left (pPGM1/*Eco*RI) or at ~60% from the left (pPGM1/*Sca*I DNA). Since the length of synapses usually did not exceed 50–100 bp, we considered the histograms of the positions of duplex crossovers as histograms of the positions of synapses.

It is important to note that the histograms of crossover position do not necessary reflect the relative efficiency of loop formation.

3. Results

3.1. Interaction of the full-length p53 with long linear DNA

Incubation of p53(1–393) with linear pPGM1/*Eco*RI or pPGM1/*Sca*I led to the formation of DNA molecules with internal loops of varying size (Fig. 1C and D). At the base of loop-constrained DNA (DNA synapse), bright spots were clearly visible. Since DNA crossings that were occasionally presented in DNA samples without addition of p53 displayed an intensity similar to that of noncrossed DNA segments (Fig. 1A and B), we inferred that these bright spots had arisen from additional interaction of uranyl cations, most probably with charged side chains of protein molecules bound with distant DNA duplexes. We characterized the efficiency of p53 interaction with linear DNA by measuring the fraction of molecules with synapsed regions and the length of synapsed regions (Table 1). Thus, at a molar protein/DNA ratio, R, equal to 4 (calculated for protein tetramers) >30% of pPGM1/*Eco*RI DNA had one or two loops, whereas at R=8, their fraction increased to ~65% leading to a synapse length of 75±35 bp. For pPGM1/*Sca*I DNA at R=4, the fraction of molecules with synapses was ~70% with a synapse length of 110±40 bp, whereas at R=8, the fraction of molecules with synapses increased to ~85% in combination with increased synapse length (135±60 bp). The minimal length of individual synapses was 30–40 bp. The length of loops also varied in the range of ~300–900 bp. In most cases, loops were intramolecular, with two duplexes in an either direct or inverted orientation.

The alignment of DNA molecules with loops (see Materials and methods) permitted the generation of position histograms of duplex synapses (Fig. 2). A large peak corresponding to the synapse occurring at p53CON is clearly visible in both histograms. The distribution of the position of the second duplex involved in synapse exhibited a broad peak located close to the p53CON site. A comparison of the histograms for both pPGM1/*Eco*RI and pPGM1/*Sca*I DNAs allowed the determination of their relative orientation and showed that the second duplex was most frequently located within the shortest *Eco*RI-*Sca*I region. We emphasize that our alignment procedure (see Materials and methods) does not ensure that the histograms

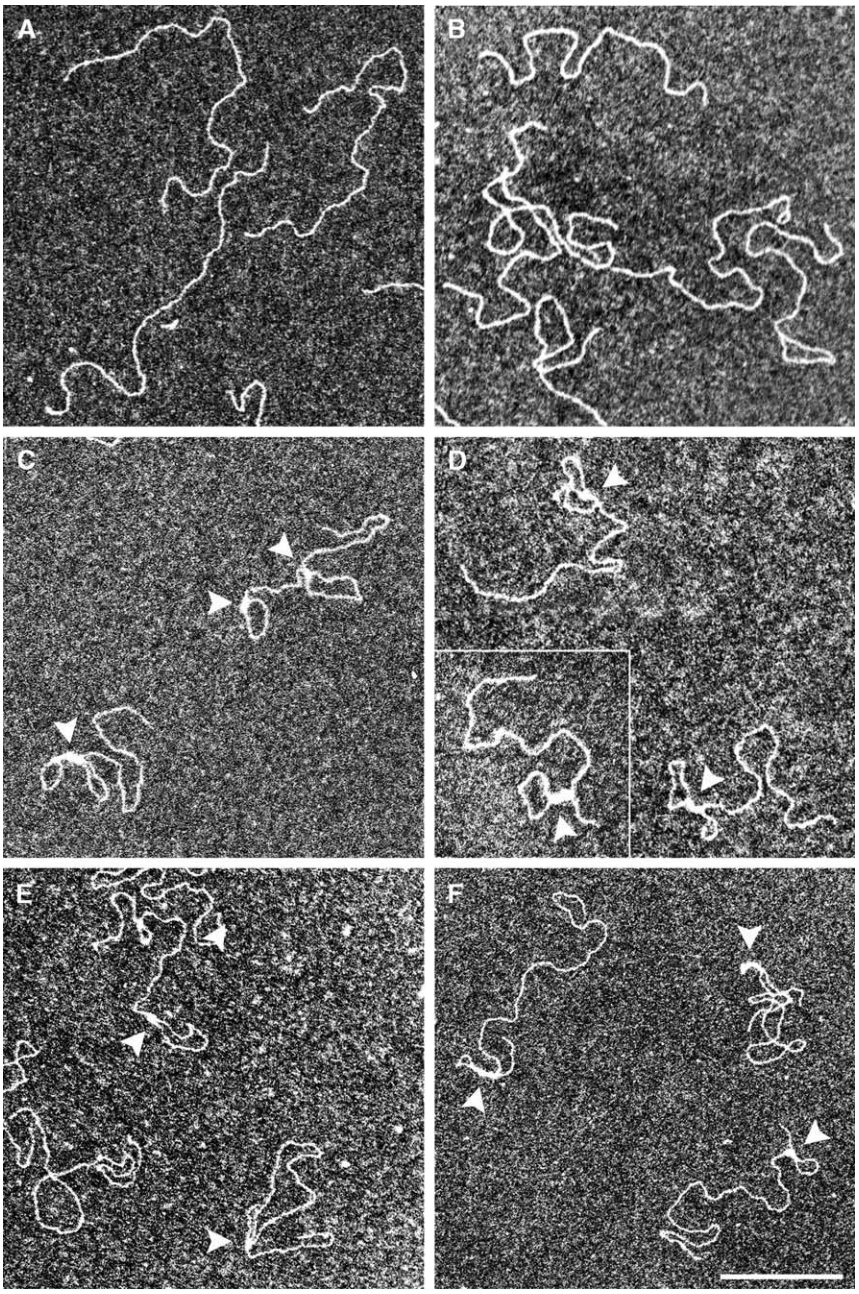

Fig. 1. Binding of bacterially expressed full-length p53 to linear DNA. Complexes prepared under the following conditions: (A) pPGM1/*Eco*RI DNA; (B) pPGM1/*Sca*I DNA; (C) pPGM1/*Eco*RI DNA+p53, *R*=8; (D) pPGM1/*Sca*I DNA+p53, *R*=8; (E) pBluescript/*Eco*RI DNA+p53, *R*=8; (F) pBluescript/*Sca*I DNA+p53, *R*=8. *R*—molar protein/DNA ratio calculated for protein tetramers. Arrowheads indicate synapsed duplexes (DNA–protein filaments). Scale bar, 200 nm.

of duplex synapses accurately reflect the relative efficiencies of the synapses.

The presence of p53CON was not a prerequisite for the synapse of DNA duplexes. Incubation of p53 with linear pBluescript DNA lacking the recognition sequence also led to the formation of intramolecular loops constrained at their base by the synapsed duplexes (Fig. 1E and F). The yield of synapse was ~60% at *R*=8, a value comparable to that of detected for the linear pGM1/*Eco*RI DNA.

3.2. Interaction of full-length p53 with scDNA of low superhelix density

Our previous data [46] and preliminary results indicated that interaction of some multimeric C-terminal fragments and bacterially expressed full-length p53 with natural scDNA ~3000 bp long, i.e., with $\Delta Lk \approx -15$, led to modulations of DNA configuration imaged as regions of lateral contact of DNA duplexes apparently linked via bound proteins (DNA–protein filaments). However, since

Table 1
Parameters of linear and superhelical DNA molecules complexed with full-length p53 measured from EM micrographs

DNA[a]	Molar protein/DNA ratio[b]	Fraction of molecules with synapses [%]	Length of synapse [bp][c]	Superhelix diameter[d] [nm]
(−) sc pPGM1	0			27 (±7)
(−) sc pPGM1	1	~40	130 (±60)	17 (±4)
(−) sc pPGM1	3	~90	340 (±165)	18 (±7)
(−) sc pPGM1	5	~95	610 (±185)	16.5 (±5)
(−) sc pPGM1	20	100	950 (±245)	14 (±6)
(+) sc pPGM1	8	~95	290 (±160)	29.5 (12)
(−) sc pBluescript	8	~100	500 (±95)	16 (±11)
(+) sc pBluescript	8	~70	230 (±120)	31 (±12)
(−) sc pPGM1	8[e]	~95	360 (±220)	21 (±9)
pPGM1/*Eco*RI	8	~65	75 (±35)	
pPGM1/*Sca*I	8	~85	135 (±60)	

[a] Linking number difference is equal to ≈−6 for (−) sc pPGM1 and (−) sc pBluescript DNAs and ≈+4 for (+) sc pPGM1 and (+) sc pBluescript DNAs.
[b] Calculated for protein tetramers.
[c] The entire length of synapsed regions (±S.D.) of a single DNA molecule corresponding to the length of DNA duplex.
[d] Supehelix diameter (±S.D.) was calculated as a weighted value using the superhelix diameter for nonlinked regions calculated using formula 4 of Boles et al. [52] and that of linked regions of ~10–12 nm.
[e] The data shown refer to the complex formed with the C-terminus p53(320–393) peptide.

this scDNA has a plectonemic configuration of a relatively small superhelix radius with a number of crossovers (nodes) ~14–15 [52], it is difficult to discriminate between DNA crossovers and regions of lateral contacts and therefore to quantify the structural alterations occurred due to protein binding. ScDNA of lower superhelix density ($|\Delta Lk| \approx 4$–6) has a larger superhelix radius [52], permitting more reliable discrimination of regions of lateral contact and DNA crossovers, especially at the lower, e.g. 10 mM, salt concentration used for mounting samples for imaging [50]. Since we did not find any significant difference in the apparent structure of the filaments and their yield when the samples were mounted in 50 or 10 mM KCl, we used the latter conditions throughout our experiments.

Incubation of p53(1–393) with negatively scDNA of low superhelix density resulted in alteration of scDNA configuration due to interaction of protein tetramers with distant (opposing) DNA duplexes. However, individual bound proteins are not observed within synapsed DNA segments (Fig. 3). We note that synapsed regions exhibited a much higher EM contrast relative to the nonsynapsed segments, similar to synapsed DNA duplexes occurring with linear DNA, implying the presence of bound protein molecules. As with linear DNA, the efficiency of interaction between scDNA and protein (reflected in alterations in scDNA configuration) can be estimated by measuring the fraction of molecules with synapsed regions, the length of synapsed regions and the apparent superhelix diameter (Table 1).

Higher protein concentration led to an increase both in the fraction of synapsed supercoiled molecules and the synapse length within a single DNA, implying a larger number of bound tetramers. At the same time, the superhelix diameter diminished from 27 nm to ~14 nm at R=20. At R>20 DNA molecules no longer had free duplex segments and tended to form higher order aggregates (not shown). The apparent width of synapsed regions was ~10–12 nm, regardless of the length of the synapse. Measurements of DNA contour length on EM micrographs did not reveal structural alterations in the duplexes constrained within the synapse.

Negative superhelicity or the presence of p53CON were not prerequisites for DNA synapse and filament formation, as similar structures were formed with positively supercoiled pPGM1 (Fig. 3F) and negatively or positively supercoiled pBluescript (Fig. 3G and H, respectively). The efficiency of p53 interaction with negatively sc pBluescript was comparable to that of negatively sc pPGM1 and slightly higher than that of their positively supercoiled counterparts (Table 1), probably due to smaller values of $|\Delta Lk|$ and/or possible modulations, although of low extent, of DNA twist.

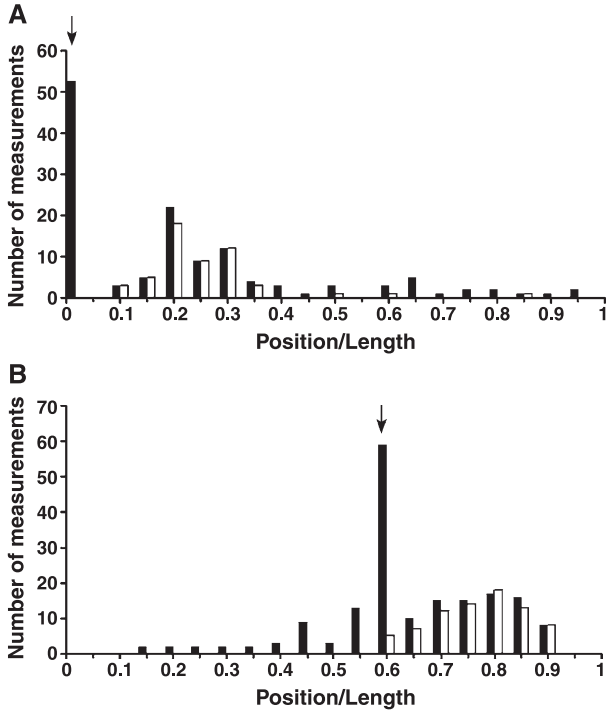

Fig. 2. Interaction of bacterially expressed full-length p53 with linear DNA. (A) Histogram of the position of synapsed duplexes (filled boxes) and the size of end loops (open boxes) obtained for pPGM1/*Eco*RI DNA (54 molecules). Position of the *Sca*I site corresponds to ~0.39. (B) Histogram of the positions of synapsed duplexes (filled boxes) and the size of loops (open boxes) associated with specific binding. The data were collected from 78 pPGM1/*Sca*I molecules. The position of the *Eco*RI site corresponds to ~0.61. Position/length corresponds to the position of duplex crossover/loop size, respectively. The number of measurements represents values binned from the 5% window of the plasmid length. Arrows (A and B) indicate the position of the p53CON.

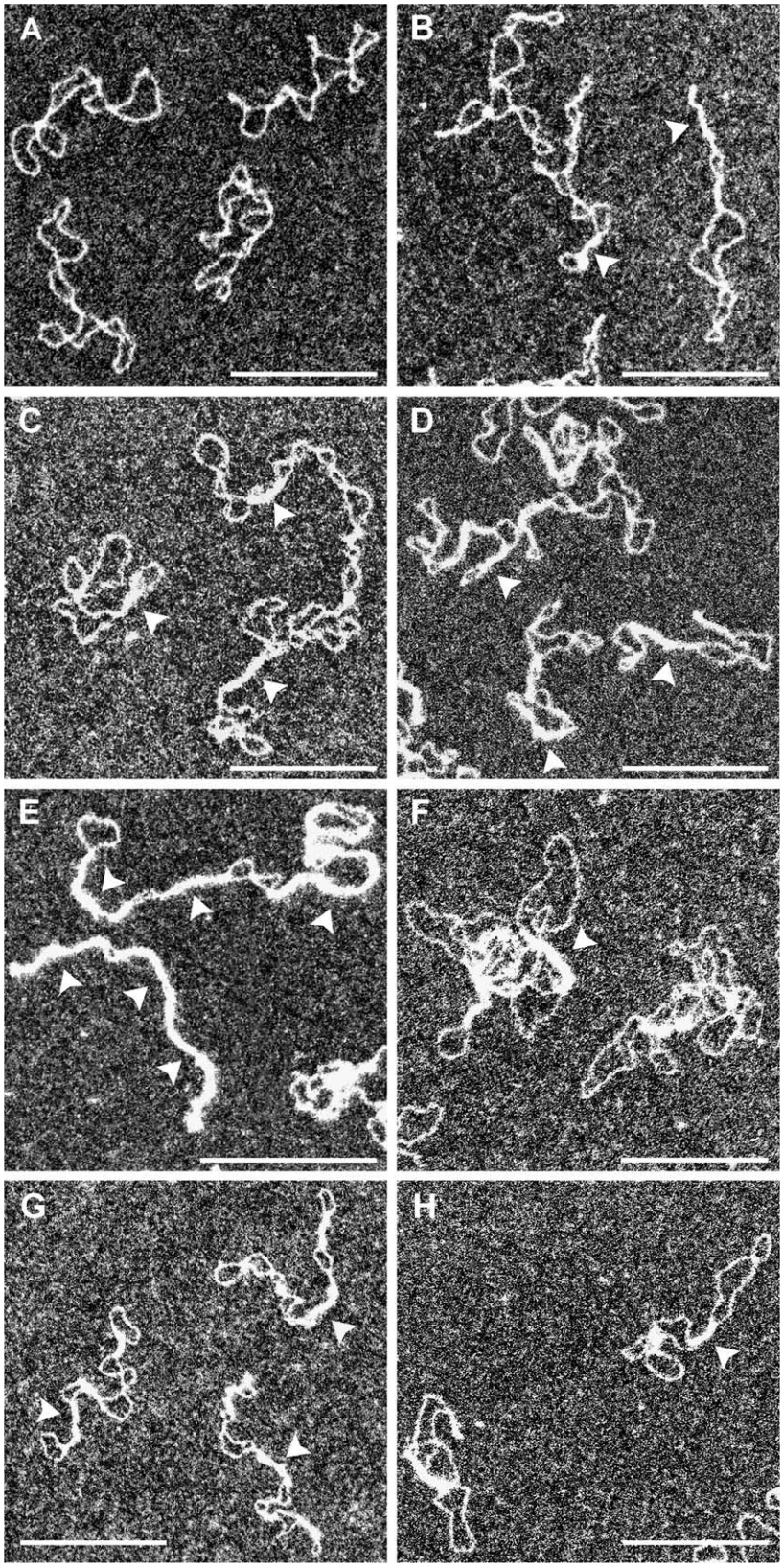

Fig. 3. Interaction of full-length p53 with supercoiled DNA. Complexes formed between p53 and negatively (A–E) and positively (F) sc pPGM1 DNAs, negatively (G) and positively (H) sc pBluescript DNAs. The molar protein/DNA ratios were 0 (A), 1 (B), 3 (C), 5 (D), 20 (E), 8 (F–H). Arrowheads indicate synapsed DNA regions (DNA–protein filaments). Scale bars, 200 nm.

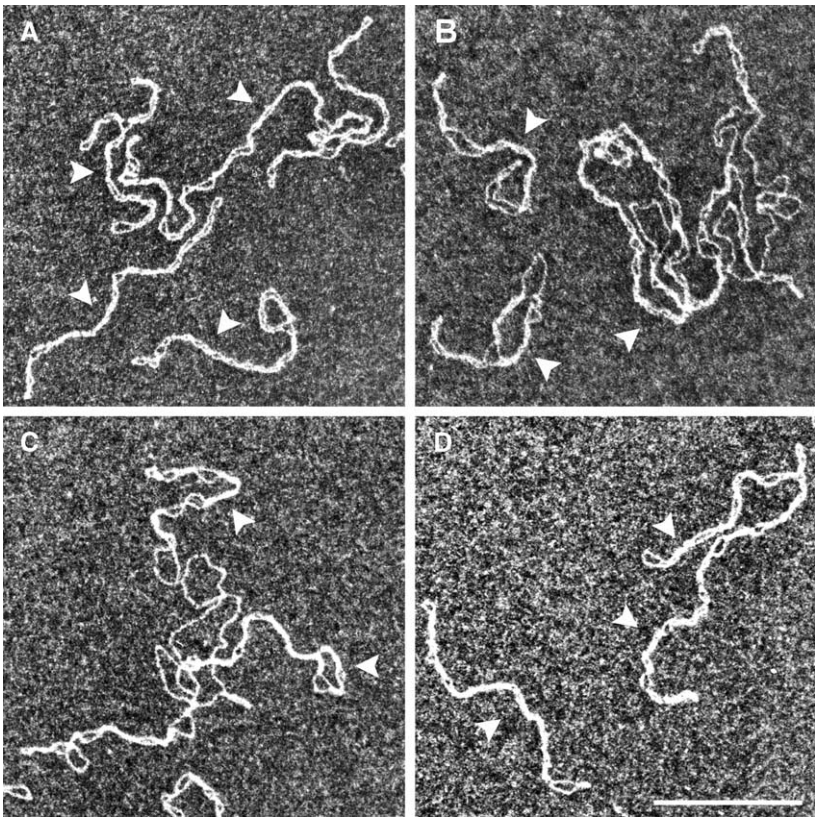

Fig. 4. Interaction of the C-terminal segment with scDNA of low superhelix density. Complexes formed between p53(320–393) and negatively (A) and positively (B) sc pPGM1 DNAs and negatively (C) and positively (D) sc pBluescript DNAs at molar protein/DNA ratio 90. Arrowheads indicate synapsed DNA regions (DNA–protein filaments). Scale bar, 200 nm.

3.3. Promoting of DNA synapse by the C-terminus

In order to evaluate the role of the C-terminus in DNA synapse under the conditions used in our experiments, we examined the interaction of p53(320–393) with linear and supercoiled DNA templates. Incubation of p53(320–393) with scDNA changed the DNA configuration dramatically, similar to the full-length protein imaged as molecules with regions of long lateral contacts exhibiting high EM contrast (Fig. 4). We ascribe the appearance of these synapsed regions to the interaction of protein tetramers with distant (opposing) DNA duplexes. The changes in scDNA configuration reflecting the efficiency of p53(320–393) interaction with DNA are summarized in Table 2. It is evident that for either supercoiled template tested, higher protein concentration led to an increase of the fraction of molecules exhibiting synapses and the corresponding length of the synapses and was accompanied by a decrease in superhelix diameter. The efficiency of interaction with negatively supercoiled DNAs was higher compared to their positively supercoiled counterparts, most probably due to the larger values of $|\Delta Lk|$. Negatively supercoiled pPGM1 exhibited

Table 2
Parameters of superhelical DNA molecules complexed with the C-terminus measured from EM micrographs

DNA[a]	Fraction of molecules with synapses [%]		Length of synapse [bp][c]		Superhelix diameter[d] [nm]		
	R=30[b]	R=90	R=30	R=90	R=0	R=30	R=90
(−) sc pPGM1	~90	100	920 (±355)	1000 (±135)	27 (±7)	20 (±7)	10 (±3)
(+) sc pPGM1	~65	100	215 (±110)	990 (±350)	53 (±18)	32 (±12)	13 (±4)
(−) sc pBluescript	~90	~100	550 (±230)	720 (±180)	22 (±5)	17 (±5)	14 (±5)
(+) sc pBluescript	~0.5	~50	105 (±40)	560 (±450)	43 (±13)	45 (±18)	20 (±7)

[a] Linking number difference for each DNA is given in the legend for the Table 1.
[b] Calculated for protein tetramers.
[c] The entire length of synapsed regions (±S.D.) of a single molecule corresponding to length of DNA duplex.
[d] Superhelix diameter (±S.D.) was calculated as a weighted value using the superhelix diameter for nonlinked regions calculated using formula 4 of Boles et al. [52] and that of linked regions of ~7–8 nm.

the highest efficiency in interaction with p53(320–393). However, this DNA was less efficiently targeted relative to the full-length protein (Tables 1 and 2).

The apparent width of synapsed regions was ~7–9 nm regardless of their length and smaller than that found for the full-length protein (~10–12 nm). Measurements of DNA contour length on EM micrographs did not reveal structural alterations in the duplexes constrained into synapse.

With linear DNA as a substrate, the yield of molecules with a synapse at the base loop-constrained DNA was very low. For R varying in a range of 20–100, less than a few percent of the molecules exhibited loops constrained by short synapsed regions (not shown).

4. Discussion

The data presented here show that the interaction of bacterially expressed full-length p53 or the C-terminal fragment p53(320–393) with dsDNA leads to structurally similar complexes characterized by the synapse of non-contiguous DNA duplexes via bound protein tetramers (DNA–protein filaments). The general mechanism of DNA synapse seems to be similar for either protein form though with some differences. We presume that the structural similarity of DNA–protein filaments observed for both proteins is mainly determined by the C-terminus, whereas the yield is highly modulated by the specific and possibly nonspecific interactions of the core domain together with DNA topology.

The protein tetramers presumably interact either simultaneously with two distant (opposing) duplexes or two bound tetramers interact with each other, thus forming the first link. Since the probability of the latter process depends on the stability of the DNA–protein complexes and the probability for the encounter of two duplexes due to thermal DNA motion, it is difficult to distinguish between the alternative mechanisms. The yield of synapsed DNA was significantly higher for supercoiled DNA relative to its linear counterpart for both protein forms analyzed. Assuming that the duplex of scDNA with fewer numbers of supercoils closely resembles that of linear DNA, the main difference between these two DNA forms is the effective local duplex concentration, reflected in the duplex-to-duplex distance (reviewed in [50]). That is, the yield of synapse is highly modulated by the probability of an encounter between the two duplexes. This is corroborated by the finding that the yield of DNA–protein filaments (using the full-length protein or the C-terminus) formed with natural negatively sc DNA either in a sc/linear competition assay[46] or in the absence of linear DNA (Cherny, unpublished) was significantly higher relative to the DNA of low superhelix density reported here.

The main difference in the interactions of the full-length p53 and its C-terminal domain is the yield of DNA synapse with both linear and supercoiled templates. We presume that the specific (and possibly non-sequence-specific) DNA-binding potential of the core-binding domain is largely responsible for this difference. There are several lines of evidence supporting this conjecture. First, short noncontiguous synapsed duplexes at the base of intra-molecular loops formed with linear pPGM1 DNA were distributed systematically. Most often, one of the two duplexes was located at or close to p53CON, whereas the second one was most frequently found within the smallest *Eco*RI-*Sca*I region of pPGM1 DNA, clearly seen for pPGM1/*Sca*I DNA in particular (Fig. 2). The length of loops was ~300–900 bp for both pPGM1/*Eco*RI and pPGM1/*Sca*I DNA, a value close to the optimal length for encounters between two distant DNA segments [53,54]. However, the nonrandom distribution of the position of the second duplex indicates that binding to preferential DNA sequences (probably p53CON-like) may play a role in loop formation. This finding implies that the specific DNA-binding activity of the core domain determines the targeting to p53CON or p53CON-like sequences. This is corroborated by the findings that (i) loops were efficiently formed with linear pBluescript DNA lacking p53CON, and that (ii) the core binding domain interacts with multiple regions of pPGM1, i.e., p53CON and those located within the smallest *Eco*RI-*Sca*I region of pPGM1 DNA, forming globular complexes (not shown).

Second, for either type of supercoiled DNA used in our experiments, similar yields of DNA synapse were detected at significantly lower protein/DNA molar ratio for the full-length protein than with the C-terminus, implying that DNA-binding activities of both the core domain and the C-terminus constituting the full-length protein act in a concerted manner. We cannot exclude a positive interference between DNA-binding potentials of the core domain and the C-terminus occurring either in solution or at the level of DNA binding. However, there is a possibility of negative interference as well. A negative influence of the core domain on the C-terminus is unlikely inasmuch as the core domain alone is incapable of promoting DNA-protein filaments. A negative influence of the C-terminus on the core domain is probable in view of the low binding affinity of the full-length protein expressed in bacteria for DNA fragments [55], compared to the higher efficiency with long DNA molecules ([45], this study). This effect is similar to that accounting for the so-called “latent” state of the full-length of p53, a feature recently put into question (reviewed in [56]). However, a negative influence of the C-terminus on the core domain DNA-binding potential contributes only slightly (if at all) and does not suppress its specific DNA-binding activity entirely. We note that a small difference in the apparent width of DNA–protein filaments formed by the C-terminus or the full-length protein (~7–9 nm and ~10–12 nm, respectively) support our proposal that the DNA-binding potentials of both domains are in concert. In this connection, it is worth noting that an interference (positive and negative) between DNA-binding potentials of the core

domain and the C-terminus has been recently reported for the full-length p53 expressed in insects [57], implying that the interaction with a noncognate sequence requires concurrent action of both domains, and the interaction with the cognate sequence increases significantly upon activation of p53 by the addition of the C-terminal antibody PAb421.

The very low yield of DNA loops upon the reaction of linear DNA with the C-terminus indicates that the interaction of protein tetramer(s) with DNA duplex(es) is weak. Specific (and possibly nonspecific) DNA-binding activity of the core domain promotes the formation of the first link most probably stabilized by several (>1) protein tetramers bound in close register as the minimal length of the synapse was 30–40 bp. A smaller yield of DNA synapse obtained for linear templates relative to their supercoiled counterparts (using the full-length protein) is likely due to increased motion of DNA chains, thus inhibiting propagation of the synapse.

Our data do not exclude the possibility of protein–protein interactions occurring between C-terminal domains from adjacently bound full-length proteins. Support of this conjecture had arisen from the observation that the interaction of the C-terminus with 35-mer (Fig. 5) or 15-mer (not shown) DNA duplexes lacking sequences matching the consensus site led to the formation of large aggregates probably similar to those reported in [58]. These aggregates were found neither for the protein alone nor for isolated DNA duplexes.

Finally, we consider the relevance of the formation of the DNA–protein filaments reported here to the biological functions of p53. In normal cells, p53 is maintained at low levels mainly by the negative regulator Mdm2, which transports to the cytoplasm ubiquitinated p53, and for subsequent degradation by the 26S proteosome [13]. Recent data led to a corrected model according to which p53 can also be degraded by the 26S proteosome in the cell nucleus [59]. Importantly, the Mdm2 gene is a transcriptional target of p53 that establishes a feedback loop, in which both the activity p53 and the expression of the Mdm2 gene are regulated. In response to stress, however, the level of p53 increases rapidly by inhibition of the ubiquitination pathway and specific phosphorylation and/or acetylation of the protein. A small amount of p53 may remain in the nucleus, presumably stored in a DNA-sequestered form. We note that preferential synapse formation with p53CON and other sequences presumably resembling p53CON implies that bound p53 should be distributed systematically over the entire genome, thereby facilitating its targeting by other proteins. It cannot be ruled out that at least a fraction of this DNA-bound p53, particularly that bound to the p53 responsive elements, can be acetylated [60], thus enhancing the response potential of the cell to the stress. Full-length p53 purified from insect cells, i.e. post-translationally modified by phosphorylation and possibly acetylation [55], does not produce DNA–protein filaments when incubated with linear or scDNA, but rather forms globular complexes interacting with p53CON [20,23] or p53CON-like sequences (Cherny, unpublished).

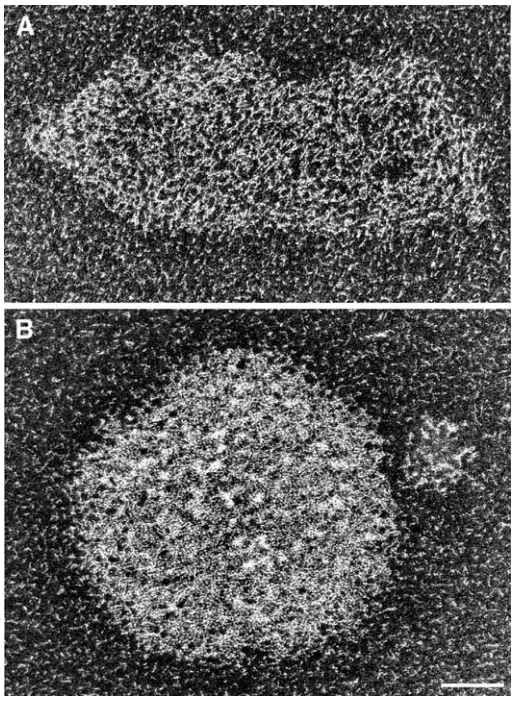

Fig. 5. Formation of large aggregates by the C-terminus p53(320–393) peptide. Aggregates formed in the presence of the p53(320–393) and a 35-mer duplex DNA. Note that a large number of individual DNA duplexes are visible in the background. Scale bar, 100 nm.

Recently, the structural flexibility of p53 due to presence of unstructured regions localized in its N- and C-terminal parts was demonstrated [16,17], thus implying the potential for a large diversity of p53 interactions with proteins and DNA. This feature can potentially account for the fibrillation of the full-length protein, particularly in view of the fact that under certain conditions the tetramerization domain [19] or the core-binding domain [18] can form amyloid-like structures. However, sequestration of p53 into DNA–protein filaments may inhibit this pathway.

The integration of p53 into DNA–protein filaments may also have a self-regulatory function independent of its transcriptional activity, e.g., suppression of homologous recombination [61,62] by virtue of inhibiting the regression of the replication fork catalyzed by human Rad51 or Rad54. p53 blocks spontaneous and RuvAB promoted branch migration of the Holliday junction and modulates the cleavage by Holliday junction resolution proteins such as RuvC [63], a role in recombinational DNA repair.

Acknowledgements

This work was supported by grants from the Grant Agency of the Czech Republic No. 301/99/D078 to J.P. and No. 301/02/0831 to E.P. was also supported by two grants

from the Grant Agency of the Academy of Sciences of the Czech Republic A4004110 and A50040513.

References

[1] K.M. Ryan, A.C. Phillips, K.H. Vousden, Regulation and function of the p53 tumor suppressor protein, Curr. Opin. Cell Biol. 13 (2001) 332–337.
[2] D.B. Woods, K.H. Vousden, Regulation of p53 function, Exp. Cell Res. 264 (2001) 56–66.
[3] A.J. Levine, p53, the cellular gatekeeper for growth and division, Cell 88 (1997) 323–331.
[4] D.W. Meek, Multisite phosphorylation and the integration of stress signals at p53, Cell. Signal. 10 (1998) 159–166.
[5] T.R. Hupp, Regulation of p53 protein function through alterations in protein-folding pathways, Cell. Mol. Life Sci. 55 (1999) 88–95.
[6] L. Jayaraman, C. Prives, Covalent and noncovalent modifiers of the p53 protein, Cell. Mol. Life Sci. 55 (1999) 76–87.
[7] C. Prives, P.A. Hall, The p53 pathway, J. Pathol. 187 (1999) 112–126.
[8] F. Janus, N. Albrechtsen, I. Dornreiter, L. Wiesmuller, F. Grosse, W. Deppert, The dual role model for p53 in maintaining genomic integrity, Cell. Mol. Life Sci. 55 (1999) 12–27.
[9] P. Chene, The role of tetramerization in p53 function, Oncogene 20 (2001) 2611–2617.
[10] J. Atz, P. Wagner, K. Roemer, Function, oligomerization, and conformation of tumor-associated p53 proteins with mutated C-terminus, J. Cell. Biochem. 76 (2000) 572–584.
[11] E. Appella, C.W. Anderson, Post-translational modifications and activation of p53 by genotoxic stresses, Eur. J. Biochem. 268 (2001) 2764–2772.
[12] D.W. Meek, Mechanisms of switching on p53: a role for covalent modification? Oncogene 18 (1999) 7666–7675.
[13] C.L. Brooks, W. Gu, Ubiquitination, phosphorylation and acetylation: the molecular basis for p53 regulation, Curr. Opin. Cell Biol. 15 (2003) 164–171.
[14] Y. Cho, S. Gorina, P.D. Jeffrey, N.P. Pavletich, Crystal structure of a p53 tumor suppressor-DNA complex: understanding tumorigenic mutations, Science 265 (1994) 346–355.
[15] A. Ayed, F.A. Mulder, G.S. Yi, Y. Lu, L.E. Kay, C.H. Arrowsmith, Latent and active p53 are identical in conformation, Nat. Struct. Biol. 8 (2001) 756–760.
[16] S. Bell, C. Klein, L. Muller, S. Hansen, J. Buchner, p53 contains large unstructured regions in its native state, J. Mol. Biol. 322 (2002) 917–927.
[17] R. Dawson, L. Muller, A. Dehner, C. Klein, H. Kessler, J. Buchner, The N-terminal domain of p53 is natively unfolded, J. Mol. Biol. 332 (2003) 1131–1141.
[18] D. Ishimaru, L.R. Andrade, L.S. Teixeira, P.A. Quesado, L.M. Maiolino, P.M. Lopez, Y. Cordeiro, L.T. Costa, W.M. Heckl, G. Weissmuller, D. Foguel, J.L. Silva, Fibrillar aggregates of the tumor suppressor p53 core domain, Biochemistry 42 (2003) 9022–9027.
[19] A.S. Lee, C. Galea, E.L. DiGiammarino, B. Jun, G. Murti, R.C. Ribeiro, G. Zambetti, C.P. Schultz, R.W. Kriwacki, Reversible amyloid formation by the p53 tetramerization domain and a cancer-associated mutant, J. Mol. Biol. 327 (2003) 699–709.
[20] J.E. Stenger, P. Tegtmeyer, G.A. Mayr, M. Reed, Y. Wang, P. Wang, P.V. Hough, I.A. Mastrangelo, p53 oligomerization and DNA looping are linked with transcriptional activation, EMBO J. 13 (1994) 6011–6020.
[21] Y. Wang, J.F. Schwedes, D. Parks, K. Mann, P. Tegtmeyer, Interaction of p53 with its consensus DNA-binding site, Mol. Cell. Biol. 15 (1995) 2157–2165.
[22] A.K. Nagaich, V.B. Zhurkin, H. Sakamoto, A.A. Gorin, G.M. Clore, A.M. Gronenborn, E. Appella, R.E. Harrington, Architectural accommodation in the complex of four p53 DNA binding domain peptides with the p21/waf1/cip1 DNA response element, J. Biol. Chem. 272 (1997) 14830–14841.
[23] D.I. Cherny, G. Striker, V. Subramaniam, S.D. Jett, E. Palecek, T.M. Jovin, DNA bending due to specific p53 and p53 core domain-DNA interactions visualized by electron microscopy, J. Mol. Biol. 294 (1999) 1015–1026.
[24] W.S. el-Deiry, S.E. Kern, J.A. Pietenpol, K.W. Kinzler, B. Vogelstein, Definition of a consensus binding site for p53, Nat. Genet. 1 (1992) 45–49.
[25] W.D. Funk, D.T. Pak, R.H. Karas, W.E. Wright, J.W. Shay, A transcriptionally active DNA-binding site for human p53 protein complexes, Mol. Cell. Biol. 12 (1992) 2866–2871.
[26] J.L. Waterman, J.L. Shenk, T.D. Halazonetis, The dihedral symmetry of the p53 tetramerization domain mandates a conformational switch upon DNA binding, EMBO J. 14 (1995) 512–519.
[27] R.A. Johnson, T.A. Ince, K.W. Scotto, Transcriptional repression by p53 through direct binding to a novel DNA element, J. Biol. Chem. 276 (2001) 27716–27720.
[28] T. Tokino, S. Thiagalingam, W.S. el-Deiry, T. Waldman, K.W. Kinzler, B. Vogelstein, p53 tagged sites from human genomic DNA, Hum. Mol. Genet. 3 (1994) 1537–1542.
[29] J.C. Bourdon, V. Deguin-Chambon, J.C. Lelong, P. Dessen, P. May, B. Debuire, E. May, Further characterisation of the p53 responsive element—identification of new candidate genes for trans-activation by p53, Oncogene 14 (1997) 85–94.
[30] H. Qian, T. Wang, L. Naumovski, C.D. Lopez, R.K. Brachmann, Groups of p53 target genes involved in specific p53 downstream effects cluster into different classes of DNA binding sites, Oncogene 21 (2002) 7901–7911.
[31] S. Lee, B. Elenbaas, A. Levine, J. Griffith, p53 and its 14 kDa C-terminal domain recognize primary DNA damage in the form of insertion/deletion mismatches, Cell 81 (1995) 1013–1020.
[32] S.T. Szak, J.A. Pietenpol, High affinity insertion/deletion lesion binding by p53. Evidence for a role of the p53 central domain, J. Biol. Chem. 274 (1999) 3904–3909.
[33] S. Lee, L. Cavallo, J. Griffith, Human p53 binds Holliday junctions strongly and facilitates their cleavage, J. Biol. Chem. 272 (1997) 7532–7539.
[34] P. Oberosler, P. Hloch, U. Ramsperger, H. Stahl, p53-catalyzed annealing of complementary single-stranded nucleic acids, EMBO J. 12 (1993) 2389–2396.
[35] G. Bakalkin, T. Yakovleva, G. Selivanova, K.P. Magnusson, L. Szekely, E. Kiseleva, G. Klein, L. Terenius, K.G. Wiman, p53 binds single-stranded DNA ends and catalyzes DNA renaturation and strand transfer, Proc. Natl. Acad. Sci. U. S. A. 91 (1994) 413–417.
[36] G. Selivanova, V. Iotsova, E. Kiseleva, M. Strom, G. Bakalkin, R.C. Grafstrom, K.G. Wiman, The single-stranded DNA end binding site of p53 coincides with the C-terminal regulatory region, Nucleic Acids Res. 24 (1996) 3560–3567.
[37] S.D. Jett, D.I. Cherny, V. Subramaniam, T.M. Jovin, Scanning force microscopy of the complexes of p53 core domain with supercoiled DNA, J. Mol. Biol. 299 (2000) 585–592.
[38] R.M. Stansel, D. Subramanian, J.D. Griffith, p53 binds telomeric single strand overhangs and t-loop junctions in vitro, J. Biol. Chem. 277 (2002) 11625–11628.
[39] E. Kim, N. Albrechtsen, W. Deppert, DNA-conformation is an important determinant of sequence-specific DNA binding by tumor suppressor p53, Oncogene 15 (1997) 857–869.
[40] E. Kim, G. Rohaly, S. Heinrichs, D. Gimnopoulos, H. Meissner, W. Deppert, Influence of promoter DNA topology on sequence-specific DNA binding and transactivation by tumor suppressor p53, Oncogene 18 (1999) 7310–7318.

[41] T. Göhler, M. Reimann, D.I. Cherny, K. Walter, G. Warnecke, E. Kim, W. Deppert, Specific interaction of p53 with target binding sites is determined by DNA conformation and is regulated by the C-terminal domain, J. Biol. Chem. 277 (2002) 41192–41203.
[42] S.J. Mazur, K. Sakaguchi, E. Appella, X.W. Wang, C.C. Harris, V.A. Bohr, Preferential binding of tumor suppressor p53 to positively or negatively supercoiled DNA involves the C-terminal domain, J. Mol. Biol. 292 (1999) 241–249.
[43] E. Paleček, D. Vlk, V. Staňková, V. Brázda, B. Vojtěšek, T.R. Hupp, A. Schaper, T.M. Jovin, Tumor suppressor protein p53 binds preferentially to supercoiled DNA, Oncogene 15 (1997) 2201–2209.
[44] V. Brázda, J. Paleček, S. Pospišilova, B. Vojtěšek, E. Paleček, Specific modulation of p53 binding to consensus sequence within supercoiled DNA by monoclonal antibodies, Biochem. Biophys. Res. Commun. 267 (2000) 934–939.
[45] E. Paleček, M. Brázdová, V. Brázda, J. Paleček, S. Billová, V. Subramaniam, T.M. Jovin, Binding of p53 and its core domain to supercoiled DNA, Eur. J. Biochem. 268 (2001) 573–581.
[46] M. Brázdová, J. Paleček, D.I. Cherny, S. Billová, M. Fojta, P. Pečinka, B. Vojtěšek, T.M. Jovin, E. Paleček, Role of tumor suppressor p53 domains in selective binding to supercoiled DNA, Nucleic Acids Res. 30 (2002) 4966–4974.
[47] G. Bakalkin, G. Selivanova, T. Yakovleva, E. Kiseleva, E. Kashuba, K.P. Magnusson, L. Szekely, G. Klein, L. Terenius, K.G. Wiman, p53 binds single-stranded DNA ends through the C-terminal domain and internal DNA segments via the middle domain, Nucleic Acids Res. 23 (1995) 362–369.
[48] P. Jackson, I. Mastrangelo, M. Reed, P. Tegtmeyer, G. Yardley, J. Barrett, Synergistic transcriptional activation of the MCK promoter by p53: tetramers link separated DNA response elements by DNA looping, Oncogene 16 (1998) 283–292.
[49] Y. Jiao, D.I. Cherny, G. Heim, T.M. Jovin, T.E. Schaffer, Dynamic interactions of p53 with DNA in solution by time-lapse atomic force microscopy, J. Mol. Biol. 314 (2001) 233–243.
[50] D.I. Cherny, T.M. Jovin, Electron and scanning force microscopy studies of alterations in supercoiled DNA tertiary structure, J. Mol. Biol. 313 (2001) 295–307.
[51] M. Brázdová, R. Kizek, L. Havran, E. Paleček, Determination of glutathione-*S*-transferase traces in preparations of p53 C-terminal domain (aa320–393), Bioelectrochemistry 55 (2002) 115–118.
[52] T.C. Boles, J.H. White, N.R. Cozzarelli, Structure of plectonemically supercoiled DNA, J. Mol. Biol. 213 (1990) 931–951.
[53] K. Rippe, P.H. von Hippel, J. Langowski, Action at a distance: DNA-looping and initiation of transcription, Trends Biochem. Sci. 20 (1995) 500–506.
[54] K. Rippe, Making contacts on a nucleic acid polymer, Trends Biochem. Sci. 26 (2001) 733–740.
[55] M. Fojta, H. Pivonkova, M. Brázdová, L. Kovarova, E. Paleček, S. Pospišilova, B. Vojtěšek, J. Kasparkova, V. Brabec, Recognition of DNA modified by antitumor cisplatin by "latent" and "active" protein p53, Biochem. Pharmacol. 65 (2003) 1305–1316.
[56] E. Kim, W. Deppert, The complex interactions of p53 with target DNA: we learn as we go, Biochem. Cell. Biol. 81 (2003) 141–150.
[57] J. Wölcke, M. Reimann, M. Klumpp, T. Göhler, E. Kim, W. Deppert, Analysis of p53 "latency" and "activation" by fluorescence correlation spectroscopy. Evidence for different modes of high affinity DNA binding, J. Biol. Chem. 278 (2003) 32587–32595.
[58] T. Yakovleva, A. Pramanik, T. Kawasaki, K. Tan-No, I. Gileva, H. Lindegren, U. Langel, T.J. Ekstrom, R. Rigler, L. Terenius, G. Bakalkin, p53 Latency. C-terminal domain prevents binding of p53 core to target but not to nonspecific DNA sequences, J. Biol. Chem. 276 (2001) 15650–15658.
[59] U.M. Moll, O. Petrenko, The MDM2–p53 interaction, Mol. Cancer Res. 1 (2003) 1001–1008.
[60] D. Dornan, H. Shimizu, N.D. Perkins, T.R. Hupp, DNA-dependent acetylation of p53 by the transcription coactivator p300, J. Biol. Chem. 278 (2003) 13431–13441.
[61] D. Yoon, Y. Wang, K. Stapleford, L. Wiesmuller, J. Chen, p53 inhibits strand exchange and replication fork regression promoted by human Rad51, J. Mol. Biol. 336 (2004) 639–654.
[62] P. Bertrand, Y. Saintigny, B.S. Lopez, p53′s double life: trans-activation-independent repression of homologous recombination, Trends Genet. 20 (2004) 235–243.
[63] V.P. Prabhu, A.M. Simons, H. Iwasaki, D. Gai, D.T. Simmons, J. Chen, p53 blocks RuvAB promoted branch migration and modulates resolution of Holliday junctions by RuvC, J. Mol. Biol. 316 (2002) 1023–1032.